Quantification and Propagation of Uncertainties in Identification of Flame Impulse Response for Thermoacoustic Stability Analysis

Shuai Guo[1]
Professur für Thermofluiddynamik,
Technische Universität München,
Boltzmannstr. 15,
Garching D-85748, Germany
e-mail: guo@tfd.mw.tum.de

Camilo F. Silva
Professur für Thermofluiddynamik,
Technische Universität München,
Boltzmannstr. 15,
Garching D-85748, Germany
e-mail: silva@tfd.mw.tum.de

Abdulla Ghani
Professur für Thermofluiddynamik,
Technische Universität München,
Boltzmannstr. 15,
Garching D-85748, Germany
e-mail: ghani@tfd.mw.tum.de

Wolfgang Polifke
Professor Professur für Thermofluiddynamik,
Technische Universität München,
Boltzmannstr. 15,
Garching D-85748, Germany
e-mail: polifke@tfd.mw.tum.de

The thermoacoustic behavior of a combustion system can be determined numerically via acoustic tools such as Helmholtz solvers or network models coupled with a model for the flame dynamic response. Within such a framework, the flame response to flow perturbations can be described by a finite impulse response (FIR) model, which can be derived from large eddy simulation (LES) time series via system identification. However, the estimated FIR model will inevitably contain uncertainties due to, e.g., the statistical nature of the identification process, low signal-to-noise ratio, or finite length of time series. Thus, a necessary step toward reliable thermoacoustic stability analysis is to quantify the impact of uncertainties in FIR model on the growth rate of thermoacoustic modes. There are two practical considerations involved in this topic. First, how to efficiently propagate uncertainties from the FIR model to the modal growth rate of the system, considering it is a high dimensional uncertainty quantification (UQ) problem? Second, since longer computational fluid dynamics (CFD) simulation time generally leads to less uncertain FIR model identification, how to determine the length of the CFD simulation required to obtain satisfactory confidence? To address the two issues, a dimensional reduction UQ methodology called "Active subspace approach (ASA)" is employed in the present study. For the first question, ASA is applied to exploit a low-dimensional approximation of the original system, which allows accelerated UQ analysis. Good agreement with Monte Carlo analysis demonstrates the accuracy of the method. For the second question, a procedure based on ASA is proposed, which can serve as an indicator for terminating CFD simulation. The effectiveness of the procedure is verified in the paper. [DOI: 10.1115/1.4041652]

1 Introduction

Predicting thermoacoustic instability remains a major concern for industry to design more reliable and efficient combustion systems. Common practices to achieve this goal include using acoustic tools such as Helmholtz solvers [1] or network models [2] to numerically solve an eigenvalue problem from which both growth rates and frequencies of the thermoacoustic modes of interest can be obtained. However, due to the nonlinear nature of the eigenvalue equation, the predicted thermoacoustic behaviors can be highly sensitive to variations [3] in geometry, boundary conditions, operating conditions, model parameters (calibrated from noisy experimental or computational data), etc. In some occasions [4], a system estimated as stable using nominal input parameters may become unstable when inputs deviate slightly from their nominal value. Consequently, uncertainty quantification (UQ) analysis, which focuses on quantifying uncertainties on output given uncertain inputs, is essential to fully account for the impact of the variable inputs from a statistical point of view and constitutes a critical step toward a more reliable thermoacoustic stability prediction.

In the process of thermoacoustic instability estimation, one of the main uncertainty sources lies in the flame model [4] which correlates the unsteady heat release rate of the flame to upstream velocity perturbations and is employed as a source term in acoustic solvers to close the thermoacoustic system [5]. Ndiaye et al. [4], Bauerheim et al. [6], Magri et al. [7], and Silva et al. [8] individually investigated the impact of flame model uncertainties on the growth rate of thermoacoustic modes of various combustors. The n–τ flame model was employed, and gain n and time delay τ were considered as uncertain input parameters in these studies. The results highlight the importance of considering flame model uncertainties in order to obtain reliable predictions of combustion instabilities.

Compared with the n–τ model used in the previous UQ studies, the finite impulse response (FIR) model represents a more sophisticated and realistic flame model. It describes flame dynamics in the time domain, facilitates direct physical interpretation of the relevant flow-flame interaction mechanisms [9], and through z-transform [10], the flame transfer function can be easily obtained and readily integrated into acoustic tools to determine thermoacoustic behaviors of the combustion system. In addition, an efficient identification procedure for impulse response models has already been established [10] which combines computational fluid dynamics (CFD) simulation and advanced system identification, and further paves the way for its convenient implementation.

However, due to the influence of the statistical nature of the system identification process, large eddy simulation (LES), low signal-to-noise ratios, finite length of CFD time series [11], etc., the estimated coefficients of the FIR model will inevitably contain uncertainties, which may be characterized by the confidence interval of each coefficient [11]. Those coefficient uncertainties will "propagate" through the thermoacoustic model and affect the output, e.g., the growth rate of the thermoacoustic modes. This aspect of the problem has not yet received enough attention, even though the FIR model has already been employed on several occasions.

[1]Corresponding author.

Manuscript received August 28, 2018; final manuscript received September 14, 2018; published online October 23, 2018. Editor: Jerzy T. Sawicki.

To do a UQ analysis with respect to this problem, two practical aspects should be addressed: first, since FIR model usually contains 15–30 coefficients, making it eligible to be classified as a high-dimensional UQ problem, a natural question is the following: is it possible to avoid high computational cost methods like Monte Carlo simulation [12], but still efficiently propagate input uncertainties to the output? Second, since generally longer simulation time yields less uncertain identification of the FIR coefficients, is it possible to have a guideline regarding how long CFD simulations should be conducted in order to achieve target confidence?

Active subspace approach (ASA) [13], an innovative approach for large-scale UQ analysis, may be able to provide solutions to the abovementioned problems. This approach identifies directions in input parameter space that give strongest variabilities of the output and compactly summarizes them as *active variables*, which form a low-dimensional representation of the original high dimensional system. Subsequently, a surrogate model (SM) can be constructed by only exploiting these active variables, allowing a much faster UQ analysis compared with direct Monte Carlo (DMC) simulations. ASA has solid mathematical foundations [14] and its capability has already been demonstrated in different research problems [15–17].

The ASA has been introduced in the field of thermoacoustic instability by Bauerheim et al. [6], who quantified uncertainties of growth rate in an annular combustor, where 38 uncertain parameters in n–τ flame model (gain n and time delay τ for each flame were considered as uncertain parameters) were reduced to only three active variables. Subsequently, low-order models were built upon these three active variables and the predicted probability of an acoustic mode to be unstable (risk factor) agreed well with the reference Monte Carlo results. Magri et al. [7] extended the work [6] by combining the ASA with an adjoint method to efficiently calculate output gradients. Different surrogate models based on active variables were compared and their respective accuracy was discussed.

In the present work, the uncertainty of modal growth rate calculation given uncertainties in the flame impulse response model is quantified. The objectives are to provide answers for the abovementioned questions, i.e., (1) How to efficiently propagate uncertainties in FIR model to determine the variation of thermoacoustic modal growth rate? (2) How to determine the length of CFD simulations required to achieve less uncertain identification of the flame impulse response model? For the first question, ASA is applied to exploit low-dimensional approximation of the original system and a 50 times faster highly accurate UQ analysis is achieved compared with the reference Monte Carlo method. For the second question, a procedure based on ASA is proposed, which can be used as an indicator for determining adequate CFD simulation time.

The novelties of the current paper are the following: (1) to our best knowledge, this is the first time that the impact of uncertainties in FIR model on thermoacoustic stability prediction is assessed; (2) we not only demonstrate the efficiency of ASA for solving the current UQ problem, we also construct an ASA-based-procedure for CFD time series length determination, which should be highly relevant for practitioners due to the high computational cost of the CFD simulation; and (3) the presented nonintrusive ASA methodology can also be applied to more complex acoustic models (thus handling more complex combustors), where classic UQ methods would be prohibitively expensive.

The paper is organized as follows. Section 2 gives an overview of the impulse response identification procedure and quantifies input uncertainties in terms of confidence intervals. Section 3 describes the investigated combustor and corresponding acoustic network model. Section 4 presents the technical details of implementing ASA. Section 5 demonstrates the effectiveness of active subspace method by comparing the results with Monte Carlo simulations. Section 6 proposes and validates the procedure used for estimating the optimal CFD simulation time. The paper closes with the main conclusions.

2 Impulse Response Model Identification

This section starts with an overview of the flame model identification procedure, followed by applying the procedure to actual LES time series data to derive the impulse response model as well as its uncertainties, the consequences of which will be investigated in the subsequent section. More comprehensive treatments of system identification as well as its uncertainties with applications in aero/thermoacoustic are given in Refs. [10], [11], and [18].

2.1 Identification Procedure. The dynamic properties of a linear time invariant single input single output system are completely characterized by its impulse response [2]. The model structure takes the following form:

$$y[k] = G(q)u[k] + e[k] \tag{1}$$

where $u[k]$, $y[k]$, and $e[k]$ represent discrete input, output, and noise term, respectively. $G[q]$ has the form

$$G(q) = h_0 + h_1 q^{-1} + h_2 q^{-2} + \cdots + h_{(L-1)} q^{-(L-1)} \tag{2}$$

where the backward-shift operator $q^{-n}x[k] = x[k-n]$ is used to refer to past inputs and outputs; L is the order of the polynomial, i.e., the "model order"; the coefficients h_k describe the response of the system submitted to unit impulse excitation, and they are the target coefficients need to be identified. Here, $G(q)$ denotes the FIR model, due to the fact that only a finite number of impulse response coefficients are considered. In the present study, procedures described in Keesman [19] are employed to identify the coefficients h_k. A brief overview is given as follows:

The FIR coefficients of the polynomial $h_0 \ldots h_{L-1}$ can be found by solving the minimization problem given by

$$\arg\min_{\theta} \sum \left(\mathbf{y} - \hat{\mathbf{y}}(\boldsymbol{\theta})\right)^2 \tag{3}$$

where $\hat{\boldsymbol{y}}(\boldsymbol{\theta})$ denotes the predicted output from the model and $\boldsymbol{\theta}$ is a place holder for all coefficients. The minimization can be achieved using the constrained least-squares approach, which is also known as a regularization algorithm

$$\hat{\boldsymbol{\theta}} = \left(\phi^{\mathrm{T}}\boldsymbol{\phi} + k\boldsymbol{I}\right)^{-1}\phi^{\mathrm{T}}\mathbf{y} \tag{4}$$

where $\mathbf{y} = [y_1, y_2, \ldots, y_n]$ is the vector containing the output at each time-step, $\boldsymbol{\phi}$ is the regressor matrix which has the form

$$\boldsymbol{\phi} = \begin{pmatrix} u[L] & u[L-1] & \ldots & u[1] \\ u[L+1] & u[L] & \ldots & u[2] \\ u[n] & u[n-1] & \ldots & u[n-(L-1)] \end{pmatrix} \tag{5}$$

the term $k\boldsymbol{I}$ represents regularization with k being the regularization parameter (set to 1 in the present study) and $\boldsymbol{I}$ being the identity matrix. Regularization can help to reduce ill-conditioning in least-squares problems and reduce covariance within estimated parameters.

Uncertainties of the estimated coefficients, which are the source of uncertainty in the focus of the present study, are represented by the covariance matrix, with its diagonal terms being the coefficient variances and its off-diagonal terms being the covariance among pairs of parameters. An estimate for the covariance matrix can be found by multiplying the Gramian matrix of ϕ with the noise variance

$$\widehat{\mathrm{cov}}(\boldsymbol{\theta}) = \left(\phi^{T}\boldsymbol{\phi} + k\boldsymbol{I}\right)^{-1}\sigma_{\varepsilon}^2 \tag{6}$$

In practice, the noise variance is estimated from the residuals $\varepsilon = \mathbf{y} - \boldsymbol{\phi}\hat{\boldsymbol{\theta}}$ as

$$\sigma_{\varepsilon}^2 \approx \frac{1}{n}\sum_{i=1}^{n}(\varepsilon_i)^2 \tag{7}$$

It is worth mentioning that the UQ analysis presented in this paper is independent of the specific identification procedure. As long as proper nominal values and covariance matrix of the FIR model parameters are provided, the UQ workflow proposed in the paper should work just fine. Details will be demonstrated in Sec. 5.

2.2 Identification Results. For the identification procedure, CFD time series of velocity perturbations u' (recorded at the burner mouth) were considered as input, i.e., $u = u'$, and global heat release rate fluctuations $\dot{Q}'$ were considered as output, i.e., $y = \dot{Q}'$. The data were obtained through LES by Tay-Wo-Chong et al. [20] and are presented in Fig. 1.

Figure 2 displays the impulse response coefficients h_k's identified by applying the procedure introduced in Sec. 2.1. $L = 16$ coefficients (i.e., impulse response coefficients h_k's) are chosen for the current model. A good practice of how to properly choose the number of coefficients L (or model order) is given in Ref. [11]. Both the nominal value and the 95% confidence interval are shown for each coefficient.

To summarize, through the identification process, nominal values as well as the covariance matrix of the FIR model coefficients are obtained. In the framework of UQ, FIR model coefficients will be treated as random variables following multivariate normal distribution.

3 Thermoacoustic Framework

In this section, details of the combustor configuration are presented first, followed by outlining the corresponding acoustic network model representation. The FIR model derived from Sec. 2.2 will be plugged into the acoustic network model to calculate the growth rate of thermoacoustic modes.

3.1 Combustor Configuration. The BRS combustor configuration investigated in the present study represents a turbulent premixed swirl burner test rig, which was experimentally investigated by Komarek and Polifke [21] and numerically investigated by Tay-Wo-Chong et al. [20]. The configuration consists of a plenum, a duct with an axial swirl generator, and a combustion chamber. It operates with an equivalence ratio of 0.77 of perfectly premixed methane-air mixture and a thermal power of 30 kW.

3.2 Thermoacoustic Modeling. In the present study, a low order acoustic network model is employed to predict thermoacoustic modes of the combustion system. The analysis is carried out in frequency domain by the assumption of linear and time-harmonic acoustics. Figure 3 displays the network model representing the burner test rig. The rig is discretized into interconnected acoustic elements, where each element is characterized by its acoustic transfer matrix, which relates the characteristic wave amplitude f and g [22], between the upstream and downstream ports of the elements. Mathematical formulations for different types of element used in this study, e.g., boundary conditions, duct, area jump, and flame, are given in Silva et al. [2].

The assembly of the individual transfer matrices yields a homogeneous system of equations for the unknown characteristic wave amplitudes. The corresponding characteristic equation is obtained by letting the determinant of the system matrix be equal to zero, and its solutions give the frequencies and the growth rates of the thermoacoustic modes.

In the present analysis, losses are not considered in modeling the area change, and zero Mach number is assumed for simplicity. The axial swirler is assumed to be acoustically transparent. The transfer matrix for the flame element is derived from linearized Rankine-Hugoniot relations. The FIR model is introduced to relate velocity fluctuations u' at the burner mouth to global heat release fluctuations $\dot{Q}'$ of the flame, thus closing the acoustic network model. Table 1 summaries geometrical and thermodynamic parameters used in the acoustic network model. Two pairs of combustion chamber length values and reflection coefficient values for the combustor exit are selected (marked as A and B in subscript), which are considered as two different cases to be submitted to subsequent UQ analysis.

4 Active Subspace Approach

This section describes the implementation of the active subspace approach in the framework of the current study. More details on its mathematical foundation as well as its implementations in other research fields are given by Constantine [14]. Figure 4 summarizes the workflow. Details in each step are given in the following:

4.1 Preparation: Inputs Transformation. The original correlated uncertain coefficients (represented in vector form, same applies after) $\boldsymbol{h} = (h_0, \ldots, h_{L-1})$ of the FIR model need to be transformed before being submitted to active subspace approach. Orthogonal transformation [23] and normalization are adopted sequentially to transform $\boldsymbol{h}$ to $\tilde{\boldsymbol{h}}$. The latter follows independent, standard, multivariate normal distribution. The inverse of the above process can convert $\tilde{\boldsymbol{h}}$ back to $\boldsymbol{h}$, which constitutes natural inputs for the acoustic network model.

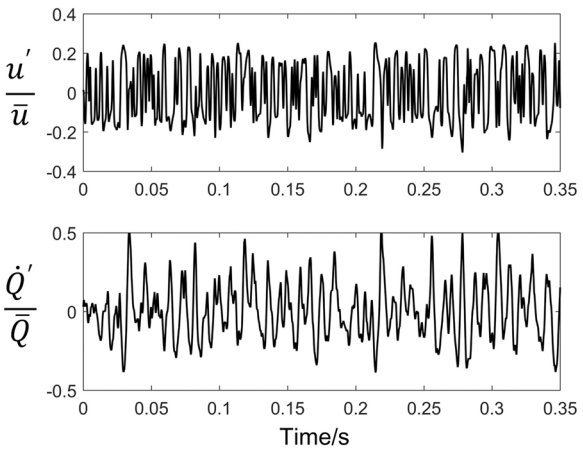

Fig. 1 Normalized velocity and global heat release rate fluctuations, the total length of the data is 350 ms

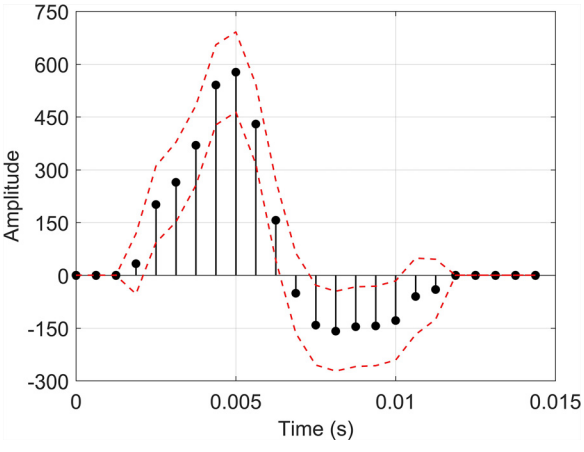

Fig. 2 Impulse response. Each discrete stem represents one coefficient h_k, upper and lower dot lines constitute the 95% confidence interval.

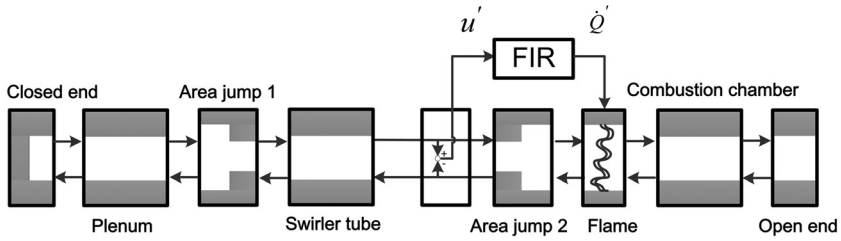

Fig. 3 Sketch of acoustic network model, flow from left to right

Table 1 Parameters of each acoustic element in the acoustic network model (Fig. 3)

Acoustic element	Parameters
Closed end	Reflection coefficient = 1
Plenum	Length = 0.17 m Sound speed = 343 m/s
Area jump 1	Area ratio = 29.76
Swirler tube	Length = 0.18 m Sound speed = 343 m/s
Area jump 2	Area ratio = 0.13
Flame	Relative temperature jump = 5.59 Ratio of specific impedances = 2.57
FIR	Impulse response model
Combustion chamber	$\text{Length}_A = 0.51$ m; $\text{Length}_B = 0.6$ m Sound speed = 880 m/s
Combustor exit	$\text{Reflection coefficient}_A = -0.9883$ $\text{Reflection coefficient}_B = -0.6351$

4.2 Data Bank Generation. We use Latin hypercube sampling to draw N samples $\widetilde{\boldsymbol{h}}^i, i = 1, 2, \ldots, N$, from an independent, standard, L-dimensional normal distribution. For each sample, we perform the inverse transformation to recover the natural inputs of the acoustic network model, then compute the corresponding growth rate. The purpose of this step is to generate a data bank for the subsequent gradient calculation.

4.3 Active Subspace Identification

(1) We use Latin hypercube sampling to draw M samples $(\widetilde{\boldsymbol{h}^i})', i = 1, 2, \ldots, M$, from independent, standard L-dimensional normal distribution. The guidance for determining a proper M value can be found in Ref. [14].

(2) For each sample $i = 1 \ldots M$, we retrieve the P nearest samples (according to Euclidean norm) and their corresponding growth rates in the data bank, and we build a local linear regression model

$$\text{Growth rate} \approx c + \sum_{j=0}^{L-1} b_j \widetilde{h}_j \tag{8}$$

where coefficients $\boldsymbol{b_i} = (b_0, \ldots, b_{L-1})_i^{\mathrm{T}}$ are taken as the gradients of growth rate against each of L coefficients at sample point i. This algorithm of calculating gradients is Algorithm 1.2 in Ref. [14].

(3) We construct the covariance matrix of the gradient vector and perform eigenvalue decomposition. Here, we use the superscript "ASA" to emphasize that the eigenvalues are obtained during the implementation of ASA, thus distinguishing them from the similar concepts of eigenvalues and eigenvectors involved in acoustic network calculation

$$\begin{gathered} \boldsymbol{C} = \frac{1}{M}\sum_{i}^{M} \boldsymbol{b_i}\boldsymbol{b_i}^{\mathrm{T}} = \boldsymbol{W}\Lambda^{\mathrm{ASA}}\boldsymbol{W}^{\mathrm{T}} \\ \Lambda^{\mathrm{ASA}} = \mathrm{diag}\left(\lambda_1{}^{\mathrm{ASA}}, \ldots, \lambda_L{}^{\mathrm{ASA}}\right) \\ \lambda_1{}^{\mathrm{ASA}} \geq \ldots \lambda_L{}^{\mathrm{ASA}} \end{gathered} \tag{9}$$

(4) We plot the eigenvalues $\lambda_1, \ldots \lambda_L$ on a log scale and look for "gaps." Here, gap refers to an order of magnitude decrease among adjacent eigenvalues. A prominent gap (as indicated in Fig. 8) in the eigenvalues indicates a separation between active and inactive subspaces, and we choose the dimension n of the active subspace to be the number of eigenvalues before the most prominent gap happens. Thus, we can make a corresponding partition of the eigenvector matrix, where $\boldsymbol{W}_1$ only contains n eigenvectors corresponding to the first n eigenvalues

$$\boldsymbol{W} = [\boldsymbol{W}_1 \quad \boldsymbol{W}_2] \tag{10}$$

The active variable vector $\boldsymbol{y}$ is defined as

$$\boldsymbol{y} = \boldsymbol{W}_1{}^{\mathrm{T}}\widetilde{\boldsymbol{h}} \tag{11}$$

Successively, entries in $\boldsymbol{y}$ represent the first active variable, the second active variable and so on. A total number of n active variables are obtained. Each active variable is expressed as a linear combination of the normalized input parameters, with the corresponding eigenvector (column vector of $\boldsymbol{W}_1$) being the linear combination coefficients. Statistically, each active variable follows independent standard normal distribution. When n is smaller than the number of input parameters, a model dimensionality reduction is achieved in the sense that subsequent surrogate model building will only need to be based upon these n active variables.

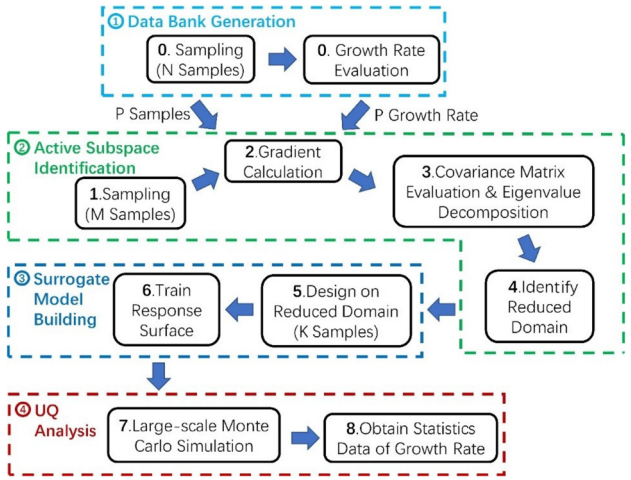

Fig. 4 Workflow of UQ based on active subspace approach

4.4 Surrogate Model Building. For each sample $i = 1 \ldots M$ in the data bank, there is a corresponding modal growth rate ω_i and a corresponding active variable vector $\boldsymbol{y}^i$. We select K representative samples from the data bank to pair the dataset $(\boldsymbol{y}^1, \omega_1) \ldots (\boldsymbol{y}^K, \omega_K)$, and we fit a regression model to express the growth rate ω as a function of $\boldsymbol{y}$.

4.5 Uncertainty Quantification. We perform standard Monte Carlo simulation on surrogate model to achieve accelerated UQ analysis. We generate S samples $\widetilde{\boldsymbol{h}_{\mathrm{MC}}}^i, i = 1, 2, \ldots, S$, from independent, standard, L-dimensional normal distribution. For each sample, $\widetilde{\boldsymbol{h}_{\mathrm{MC}}}^k$ among $\widetilde{\boldsymbol{h}_{\mathrm{MC}}}^1 \ldots \widetilde{\boldsymbol{h}_{\mathrm{MC}}}^S$ calculates corresponding $\boldsymbol{y}_{\mathrm{MC}}{}^k$ as

$$\boldsymbol{y}_{\mathrm{MC}}{}^k = \boldsymbol{W}_1{}^{\mathrm{T}} \widetilde{\boldsymbol{h}_{\mathrm{MC}}}^k \tag{12}$$

then the corresponding growth rate $\omega_{\mathrm{MC}}{}^k$ can be directly computed through the surrogate regression model. Based on the obtained growth rate dataset $\omega_{\mathrm{MC}}{}^1 \ldots \omega_{\mathrm{MC}}{}^S$, a probability density function (PDF) regarding the growth rate can be constructed and relevant statistical indices can be extracted.

Figure 5 compares the ASA against DMC. To summarize, first, ASA invokes only a small number of acoustic solver calculations to identify a low-order structure within the original thermoacoustic system. Second, it replaces this expensive thermoacoustic system with a cheap algebraic surrogate model. Third, standard Monte Carlo simulations are applied only on the surrogate model with negligible cost through which a much faster UQ analysis is achieved. The most computational intensive step of ASA lays in Sec. 4.2, which requires a number of full-accuracy acoustic network calculations. For the terminology, even though Monte Carlo method is also adopted in the framework of ASA, we refer to the whole chain of analysis as ASA, while referring to the benchmark method as DMC.

5 Uncertainty Quantification Analysis

This section aims to answer the first question proposed in the introduction, i.e., to demonstrate that the ASA can indeed effectively achieve reduction of parameter dimensionality and significantly reduce the computational cost of UQ analysis, while maintaining high accuracy. Two cases with different values of combustion chamber length and reflection coefficient at combustor exit (cases A and B, as indicated in Table 1) are considered.

5.1 Thermoacoustic Mode Specification. Figure 6 shows the thermoacoustic modes up to 500 Hz for both cases, when the nominal coefficient values of the FIR model are used for acoustic network calculation. This analysis is a deterministic analysis, meaning no uncertainties are considered in the input parameters. Highly damped modes are also ignored. According to the convention adopted in the current investigation, modes with growth rates larger than zero are considered unstable.

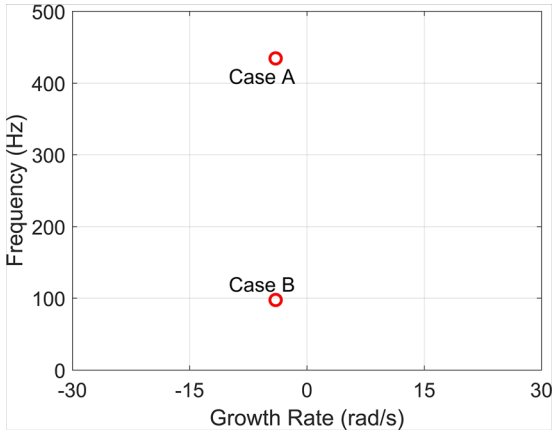

Fig. 6 Eigenmodes from deterministic analysis. For case A, the dominant mode is quarter wave mode [22], with a frequency of 434.2 Hz and a growth rate of −4 rad/s. For case B, the dominant mode is intrinsic mode [22], with a frequency of 97.5 Hz and a growth rate of −4 rad/s.

For both cases, the dominant modes are relatively close to the stability limit and may be calculated as unstable when uncertainties in FIR model coefficients are taken into account. Therefore, subsequent UQ analysis will only focus on these modes.

5.2 Direct Monte Carlo Results. Monte Carlo simulation is the classic method to propagate uncertainties from inputs to outputs. To implement the method in the present study, samples of FIR coefficients are drawn from the joint probability distribution characterized by the expectation value and the covariance matrix, which are obtained from the system identification. Each of these samples, seen as a FIR model perturbed around the model with nominal coefficient values, is subsequently fed into the acoustic network, and the corresponding perturbed modal growth rate is recorded. Based on the results of 20,000 times of acoustic network calculations, various statistical indices of the modal growth rate can be extracted.

Results of DMC are presented in Fig. 7 where contours of the joint probability density function of the modal frequency and growth rate are shown, which are constructed by 20,000 times of

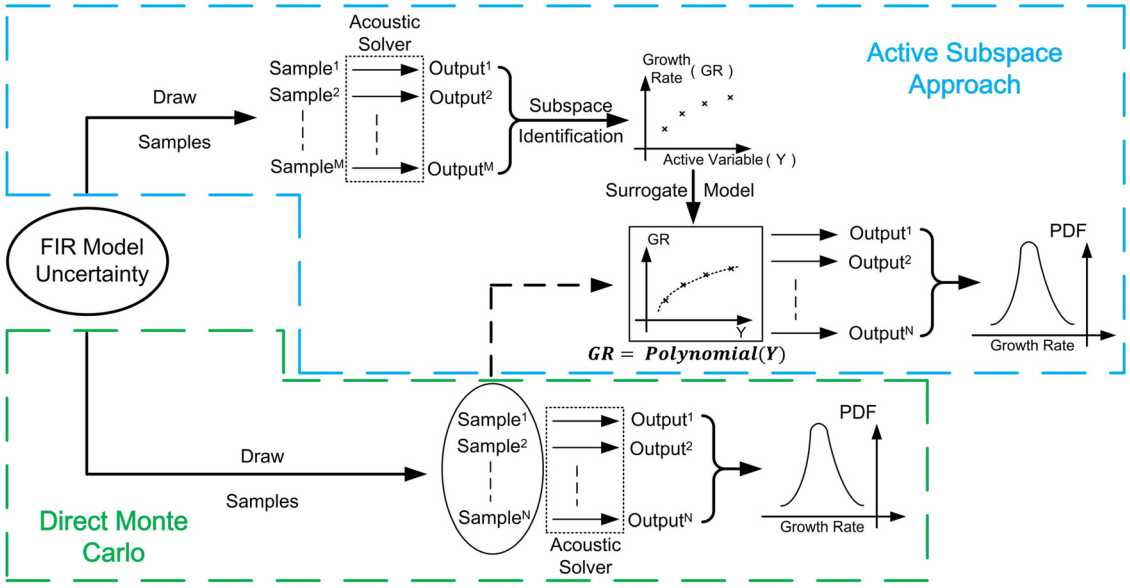

Fig. 5 Active subspace approach and DMC simulation

acoustic solver calculations. First, uncertainties in FIR model coefficients have significant impact on the predicted thermoacoustic stability in both cases, leading to 95% confidence intervals of (-4.03 ± 11.03) rad/s for case A and (-4.04 ± 7.15) rad/s for case B, respectively, in terms of the marginal distribution of the modal growth rate. Second, eigenmodes have a higher possibility to appear close to the nominal value, while lower probability is observed as eigenmodes move away from the center. Third, even though in both cases the modes have a growth rate of -4 rad/s according to the deterministic analysis, their standard deviations are different (5.63 rad/s for case A and 3.65 rad/s for case B) for the given amount of uncertainty. Those facts highlight the insufficiency of deterministic analysis.

5.3 Active Subspace Results. To accelerate the above UQ analysis, ASA is implemented for both cases with $N = 400$, $M = 110$, $P = 50$, $K = 5$, and $S = 20{,}000$, which, according to the convergence study, are considered to be sufficient.

Following the procedure outlined in Sec. 4, for each case, the covariance matrix of the gradient vector is constructed and eigenvalue decomposition is performed. Figure 8 shows the obtained eigenvalues in descending order. For both cases, since there exists a prominent gap between the first and the second eigenvalue, it is suggested that only the first eigenvector (corresponding to the largest eigenvalue in Figs. 8(*a*) and 8(*b*)), shown in Fig. 9, needs to be retained to form a single active variable, individually. Therefore, the dimensionality of the UQ problem shrinks from 16 (16 FIR model coefficients) to 1 (one active variable).

Two remarks worth mentioning here: (1) It is not a coincidence that both cases admit a one-dimensional structure. Our ongoing research has already mathematically proved that to first-order approximation the causal relationship between variations of FIR model coefficients and variations of model growth rate should collapse on a 1D subspace (i.e., a single active variable). This argument does not rely on the ASA implementation that the present manuscript relies on and is valid under the condition that the uncertainty level of the FIR model coefficients (represented as the ranges of coefficient confidence interval) is moderate. This condition is certainly fulfilled in the present case; for the FIR model investigated in our current paper, its uncertainty level can already be considered large (the maximum ratio of coefficient standard deviation to coefficient mean can be as large as 130%). These results of the physical interpretation of the active variable as well as the pertinent analytical derivations can be found in Ref. [12]. (2) The components of the first eigenvector in case B (Fig. 9(*b*)) are different from the counterparts in case A (Fig. 9(*a*)). This is expected for the following reason: according to Constantine [17], components of the eigenvector, which are also the coefficients of the linear combination that forms the active variable, reflect the sensitivity of the output (mode growth rate) against each input (individual FIR model coefficient h_k). Since two cases deal with

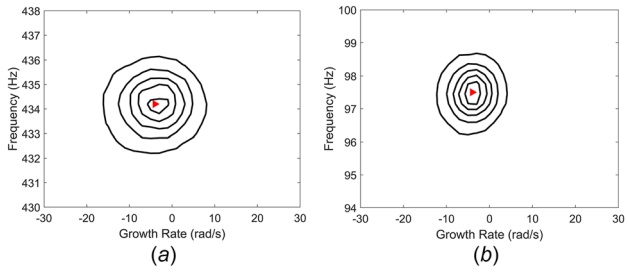

Fig. 7 Contour plot of the joint PDF of the modal growth rate and frequency. The contours (from outside to inside) correspond to 10%, 30%, 50%, 70%, and 90% of the maximum probability. The triangle is the deterministic solution (same as Fig. 6). Statistics regarding the marginal distribution of the modal growth rate are presented in Table 2: (*a*) case A and (*b*) case B.

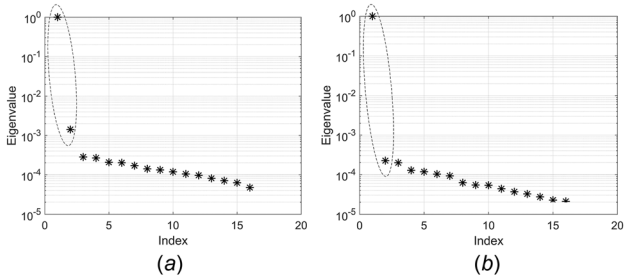

Fig. 8 Eigenvalues in λ^{ASA} in descending order. The prominent gap between the first and second eigenvalues indicates that a one-dimensional subspace exists: (*a*) case A and (*b*) case B.

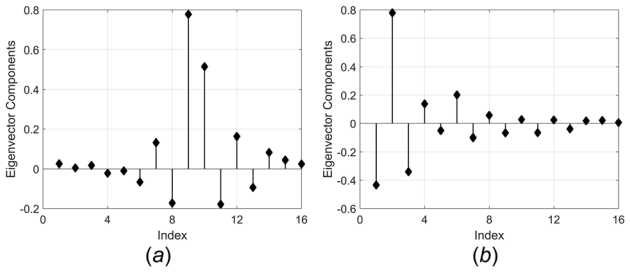

Fig. 9 Components of the first eigenvector in W_1, which will be used as the linear combination coefficients to form the single active variable: (*a*) case A and (*b*) case B

two different combustor boundary conditions and thermoacoustic modes, the sensitivity of the modal growth rate against FIR model coefficients should be different, which explains the difference between Figs. 9(*a*) and 9(*b*).

For each sample generated in Sec. 4.2, on the one hand, we have already calculated its corresponding modal growth rate value; on the other hand, through Eq. (11), we can calculate its corresponding active variable value. By checking the relation between these two values for each sample, which is plotted in Fig. 10, it is possible to verify if a one-dimensional approximation exists. It can be seen clearly from Fig. 10 that a strong univariate trend is present and it confirms that ASA method does recover an accurate one-dimension approximation of the original system. In the present study, we construct a quadratic regression model to map from the active variable value to the modal growth rate value for each case and later large-scale Monte Carlo simulations are performed on these regression models.

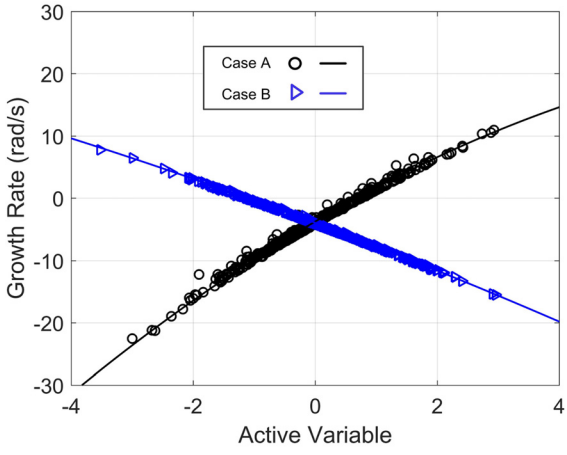

Fig. 10 Sufficient summary plot of the modal growth rate against active variable for each sample. We fit a quadratic function to link active variable and modal growth rate for each case.

Figure 11 compares the results between ASA and DMC. The PDF generated by the regression model matches well with the distribution given by the DMC, demonstrating again that one-dimensional structure identified by ASA can mimic the behaviors of the original high dimensional system with high accuracy.

5.4 Approach Assessment. In terms of computational cost, DMC requires 20,000 acoustic solver calculations for each case to obtain fully converged statistical indices. This relatively high computational cost is caused by the slow convergence of random sampling adopted in DMC. In contrast, the ASA replaces the original high dimensional system (16 parameters) with an algebraic one-dimensional model (one active variable), where subsequently UQ analysis will be applied on with negligible computational cost. As a result, only a total number of $N = 400$ acoustic solver calculations (for data bank generation) are needed for a converged and accurate UQ analysis, which significantly accelerates the analysis process.

Finally, statistical indices of modal growth rate distributions predicted by ASA are compared with DMC in Table 2. Here, RF stands for risk factor, which is defined as the probability that a mode is unstable [4] and its expression is shown in Eq. (13). To summarize, it can be concluded that ASA can indeed significantly reduce the computational cost of UQ analysis while maintaining high accuracy, which confirms the results of Bauerheim et al. [6]

$$\mathrm{RF}(\%) = 100 \int_0^\infty \mathrm{PDF}(\omega) d\omega \tag{13}$$

It is worth mentioning that a rather simple yet practical acoustic network model is adopted in the current study, where DMC is entirely feasible to obtain the PDF of the modal growth rate. For more computational intensive acoustic models, like the ones characterized by the Helmholtz equation or the Linearized Navier–Stokes equation, DMC would no longer be an option, then ASA really pays off.

6 Optimum Computational Fluid Dynamics Time Length Estimation

This section aims to answer the second question proposed in the introduction, i.e., to find a practical procedure to estimate the length of CFD time series required for FIR model identification, so that final uncertainties in modal growth rate are within a desired range. In this section, first, motivation for seeking this procedure and feasible solutions are discussed; second, a case study is presented to demonstrate the argument; and finally, steps for implementing the procedure are summarized.

6.1 Motivation and Solutions. Generally speaking, identification of FIR model from longer CFD time series yields smaller variance of model coefficients, thus leading to a less uncertain estimation of the modal growth rate. From Sec. 5, we can see that the FIR model identified from 350 ms's LES time series contains

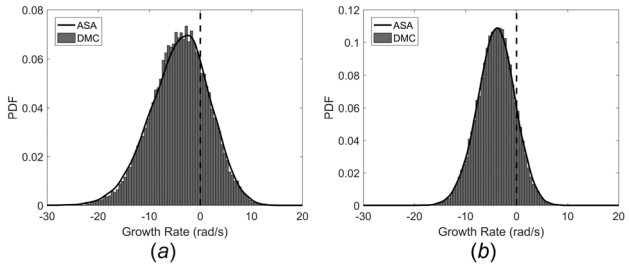

Fig. 11 Probability density function of thermoacoustic growth rate of dominant mode produced by ASA and DMC: (*a*) case A and (*b*) case B

Table 2 Statistical indices comparison: mean, standard deviation, and RF

	Case A		Case B	
	DMC	ASA	DMC	ASA
Mean	−4.03	−4.04	−4.04	−4.03
StDev	5.63	5.78	3.65	3.69
RF	24.1%	25.1%	13.3%	13.7%

relatively large uncertainty, leading to a 24% of risk factor of the modal growth rate for case A. Therefore, to obtain a more robust estimation of the modal growth rate, longer LES time series may be necessary. Then, exactly how much longer time series data are required so that a satisfactory reduction of the uncertainty of the modal growth rate estimation can be achieved? Is it possible to propose a procedure to estimate this time length?

A feasible procedure to achieve this is illustrated in Fig. 12: for an ongoing unsteady CFD run, whenever the simulation has progressed a fixed period of time, estimate FIR model coefficients as well as their uncertainties, employ ASA to evaluate uncertainty in the modal growth rate, terminate this process when the uncertainty fulfills accuracy requirement.

Compared with performing DMC every time, obviously the abovementioned procedure can significantly reduce the computational cost. However, the identification of low-dimensional structure and construct surrogate model from time to time still persist as tedious work. Then, is it possible to further improve the procedure to make it more efficient?

As a matter of fact, we argue that as long as the number of FIR model coefficients is kept constant, it is reasonable to assume that the surrogate model, which is obtained by applying ASA on the FIR model identified from t_0 length of time series (as indicated in Fig. 12), can be used without modification for subsequent UQ calculations when longer CFD time series are available. Therefore, only once ASA implementation is needed for the whole process. The rationality of this assumption lays in the fact that this surrogate model quantitatively describes the physical relations between the FIR model coefficients (varied within the individual confidence interval) and the modal growth rate. As longer time series ($t_0 +$ iterations Δt) is put into use, the newly obtained confidence

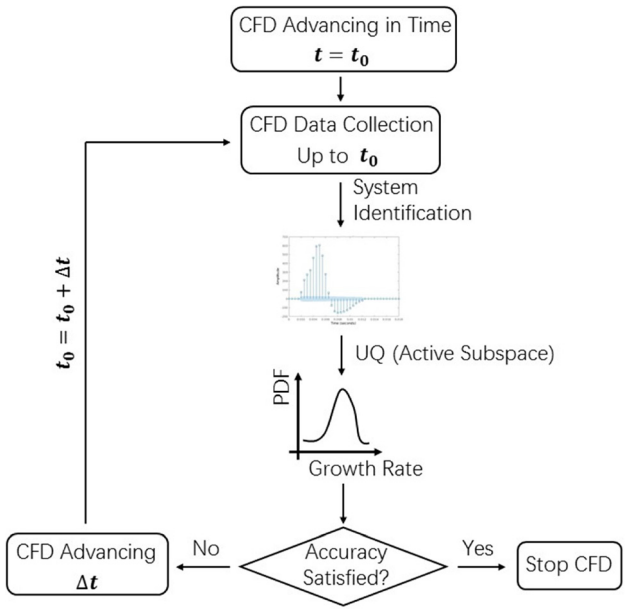

Fig. 12 A feasible workflow for estimating appropriate CFD simulation time to achieve predefined confidence requirements

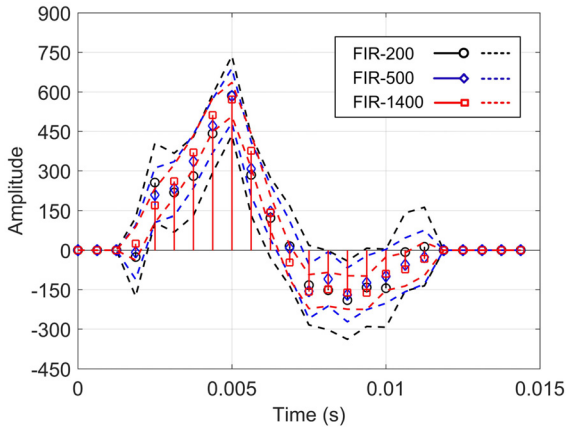

Fig. 13 Finite impulse response models identified from time series of different length. Here, confidence intervals (represented by ±3 standard deviations) of FIR model coefficients become narrower as length of time series increases.

intervals will become narrower and covered by the previous confidence intervals based on t_0 length of time series. Automatically, this same surrogate model remains valid, thus, eliminating the need for further ASA implementation.

6.2 Case Study. Case A in Sec. 5 is restudied here, but with three versions of 16-coefficient FIR model identified using different lengths of time series data (as shown in Fig. 13). Here, instead of actual LES data, synthetic time series are employed, which allows a longer time length for better illustration. To generate the synthetic time series, the FIR model in Fig. 2 is used as the reference FIR model, and a broadband velocity signal u' is applied to excite the FIR model to obtain the heat release perturbation. A Gaussian distributed white noise is added afterward to finally generate the corresponding synthetic heat release signal Q'. A similar approach to generate synthetic data for system identification is employed by Jaensch et al. [24].

The workflow for this case study is outlined in Fig. 14, where ASA will only be implemented once, on the impulse response model ("FIR-200") identified from 200 ms of synthetic time series. The goal is to prove that the derived surrogate model can also be used for UQ evaluation when longer time series are considered, thus making it possible for performing UQ analysis on the fly during an on-going CFD run. The obtained two PDFs of modal growth rate in Fig. 14 will be compared with corresponding DMC results to assess the accuracy.

The first step is to apply ASA on "FIR-200" model. Here, we assume that the FIR-200 model coefficients are independent and only the diagonal terms of the covariance matrix of FIR-200 are used for generating samples. The rationality of this treatment is the following: we are aiming to construct a surrogate model, which, in the end, forms a direct mapping from the values of h_i's in $\boldsymbol{h}$, to the value of the modal growth rate, i.e., Growth Rate $=$ surrogate$(\boldsymbol{h})$ $=$ surrogate$(h_0, h_1, \ldots, h_{15})$, and remains valid in the domain determined by the confidence interval of each FIR-200 model coefficient. To achieve this goal, we need to generate samples of $\boldsymbol{h}^i, i = 1, \ldots, N$ that can cover this domain, and the information contained in the diagonal terms of the covariance matrix is enough to guide us in generating representative samples. The benefit of this treatment is that the mathematical manipulation can be significantly simplified where no orthogonal transformation (Sec. 4.1.1) is required.

Figures 15 and 16 demonstrate the corresponding results of ASA. As expected, a one-dimensional structure is identified and only the first eigenvector needs to be retained to form a single active variable. Figure 16 plots the modal growth rate against the active variable, which further confirms that modal growth rate can be approximated as a univariate function of the active variable. We notice that the eigenvector shown in Fig. 15(*b*) is different from Fig. 9(*a*). This is because, in Fig. 15(*b*), the eigenvector is with respect to the original h_i's, while in Fig. 9(*a*) the eigenvector is with respect to the transformed $\tilde{h}_i$'s.

The second step is to obtain the corresponding surrogate model, which is expressed as

$$Y = a_1\left(\frac{h_1 - \bar{h}_1}{\sigma_1}\right) + a_2\left(\frac{h_2 - \bar{h}_2}{\sigma_2}\right) + \cdots + a_{16}\left(\frac{h_{16} - \bar{h}_{16}}{\sigma_{16}}\right) \tag{14}$$

$$\text{Growth rate} = \beta_0 + \beta_1 Y + \beta_2 Y^2 \tag{15}$$

where Y is the active variable and a_i's are the entries in the eigenvector (shown in Fig. 15(*b*)). h_i's represent FIR model coefficients, and $\bar{h}_i$'s and σ_i's are the nominal values and standard deviations of FIR-200 model coefficients, resectively. β_i's denote the polynomial coefficients of the quadratic regression model we fit.

The third step is to use the obtained surrogate model to perform UQ analysis against "FIR-500" model and "FIR-1400" model. For both models, full covariance matrices are considered. At this point, it is worth mentioning that since the surrogate model forms

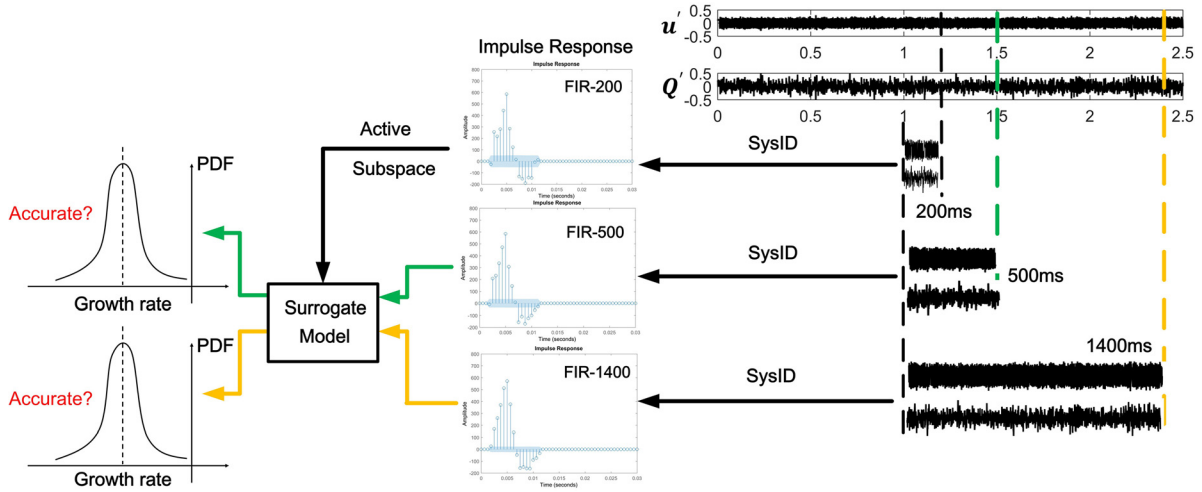

Fig. 14 200 ms, 500 ms, and 1400 ms of synthetic series are used to identify "FIR-200," "FIR-500," and "FIR-1400" model, respectively. Active subspace approach will only be implemented once on "FIR-200" to derive the SM.

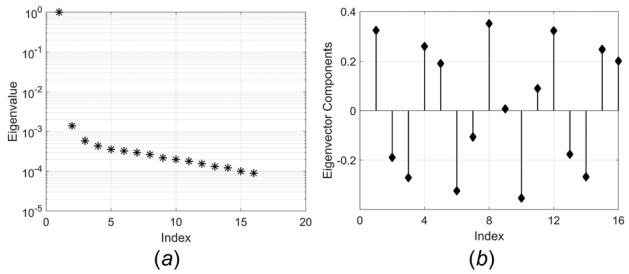

Fig. 15 (*a*) Eigenvalues in descending order and (*b*) components of the first eigenvector

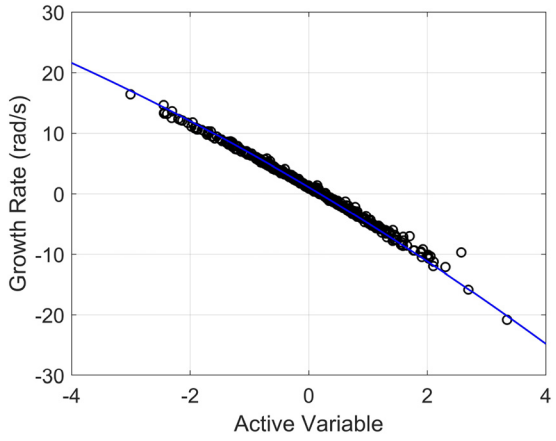

Fig. 16 Sufficient summary plot of the modal growth rate against active variable. A quadratic regression model is fitted to describe the relation between active variable and modal growth rate.

a direct link from $\boldsymbol{h}$ to modal growth rate, this surrogate model would not concern about how exactly the samples $\boldsymbol{h}^i$ are generated. As long as $\boldsymbol{h}$ with suitable values of h_i's (suitable means values of h_i's are within the confidence intervals of FIR-200 model coefficients) is provided, the calculation of modal growth rate is straightforward. Therefore, in practice, we generate samples using the full covariance matrices of FIR-500 and FIR-1400 models, and we fed those samples directly into the obtained surrogate model (Eqs. (14) and (15)) to calculate the corresponding PDF of modal growth rate. We emphasize that it is not necessary to implement ASA anymore.

Results comparison are summarized in Fig. 17 and Table 3. It can be seen that the generalized surrogate model built upon the uncertainty information of FIR-200 model is also able to achieve successful UQ analysis when new uncertainty information is provided, thus confirming our previous arguments.

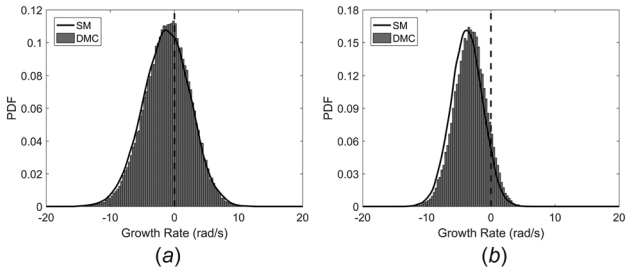

Fig. 17 Comparison of PDF results produced by SM and DME, considering the uncertainty information of (*a*) "FIR-500" model and (*b*) "FIR-1400" model

Table 3 Statistical indices comparison: mean, standard deviation, and RF

	FIR-500		FIR-1400	
	DMC	SM	DMC	SM
Mean	−1.08	−1.25	−3.23	−3.76
Std	3.57	3.68	2.48	2.45
RF	38.8%	37.3%	9.5%	6.2%

Procedure: Estimating Optimal CFD Time Length for FIR Identification

Unsteady CFD finished to t_0
Set $t_{current} = t_0$
Set *Flag* equals to 0
While (*Flag* equals 0)
  Data = CFD (0: $t_{current}$) # Prepare available CFD time series
  [*FIR.nominal*, *FIR.uncertainty*] = System Identification (*Data*)
  if ($t_{current}$ equals t_0)
    # Construct generalized surrogate model, only perform once
    Surrogate Model = Active Subspace (*FIR.nominal*, *FIR.uncertainty*)
    # Employ generalized surrogate model to perform fast UQ analysis
    Growth Rate PDF = *Surrogate Model*(*FIR.nominal*, *FIR.uncertainty*)
  else
    Growth Rate PDF = *Surrogate Model*(*FIR.nominal*, *FIR.uncertainty*)
  end
  if (*Growth Rate PDF* satisfies **Pre-defined Goal**)
    Flag = 1
  else
    CFD Advancing Δt
    $t_{current} = t_{current} + \Delta t$
  end
end

Fig. 18 The proposed procedure for estimating CFD time length for FIR identification

6.3 Procedure Implementation. Figure 18 provides the pseudocode for procedure implementation. A good starting point for t_0, which is the minimum CFD time series required before executing the procedure, would be at least ten times the length of the impulse response [25].

7 Conclusions

Based on active subspace approach, UQ analyses regarding the impact of FIR model uncertainties on thermoacoustic instabilities are performed in the present paper. Answers for two practical questions are provided: First, "How to efficiently propagate uncertainties from a FIR model for the flame dynamics to the modal growth rate of the system?," the current research indicates that active subspace approach can achieve highly efficient and accurate UQ analysis by constructing and exploiting a one-dimensional surrogate model. Compared with direct Monte Carlo, 50 times faster UQ analysis was recorded with the cases considered in the paper. For the second question, i.e., "Which length of CFD time series is required for a desired confidence of system identification?," the current research further explored the potential of active subspace approach and proposed a ready-to-implement procedure in pseudocode form. A case study was performed which confirmed the effectiveness of the procedure. It can also be seen as a demonstration of the procedure workflow.

Compared with the previous achievements in the field of UQ analysis of thermoacoustic instabilities, the novelties of the current work reflect in: (1) to our best knowledge, this is the first time that the impact of uncertainties in flame FIR model, which

represents a sophisticated and realistic time-domain model of flame dynamics, on thermoacoustic stability prediction has been assessed; (2) we have gone one step further by proposing an ASA-based procedure to effectively determine the length of CFD simulation that is required to achieve FIR model identification with a desired level of uncertainty. This should be highly relevant for practitioners due to the high computational cost of the CFD simulation; (3) the presented nonintrusive ASA methodology can also be applied to more complex acoustic models (thus handling more complex combustors), where classic UQ methods would be prohibitively expensive.

Further study will include more sources of uncertainty, e.g., boundary conditions and model parameters, and investigate their combined effects in thermoacoustic instability prediction [26].

Acknowledgment

S. Guo is grateful for the financial support from doctoral scholarship of Chinese Scholarship Council. W. Polifke and C. Silva are grateful to the 2014 Center for Turbulence Research Summer Program (Stanford University), where discussions with Michael Bauerheim and Franck Nicoud instigated the ideas developed in this study.

Funding Data

- China Scholarship Council (No. 201606830045).

Nomenclature

ASA = active subspace approach
DMC = direct Monte Carlo
FIR = finite impulse response
$\boldsymbol{h}$ = FIR model coefficients in vector form
$\widetilde{\boldsymbol{h}}$ = transformed FIR model coefficients in vector form
h_i = FIR model coefficient
K = number of samples in ASA for surrogate model building
L = FIR model order
M = number of samples in ASA for active subspace identification
N = number of samples in ASA for data bank generation
P = number of samples in ASA for gradient calculation
PDF = probability density function
$\dot{Q}'$ = heat release rate fluctuation
RF = risk factor
S = number of samples in ASA for Monte Carlo simulation
u = input for system identification
UQ = uncertainty quantification
u' = velocity fluctuation
$\boldsymbol{W}_1$ = matrix with column vectors being the eigenvectors that form the active variables
y = output for system identification
$\boldsymbol{y}$ = active variable vector

References

[1] Nicoud, F., Benoit, L., Sensiau, C., and Poinsot, T., 2007, "Acoustic Modes in Combustors With Complex Impedances and Multidimensional Active Flames," AIAA J., **45**(2), pp. 426–441.
[2] Silva, C. F., Emmert, T., Jaensch, S., and Polifke, W., 2015, "Numerical Study on Intrinsic Thermoacoustic Instability of a Laminar Premixed Flame," Combust. Flame, **162**(9), pp. 3370–3378.
[3] Magri, L., and Juniper, M. P., 2013, "Sensitivity Analysis of a Time-Delayed Thermo-Acoustic System Via an Adjoint-Based Approach," J. Fluid Mech., **719**, pp. 183–202.
[4] Ndiaye, A., Bauerheim, M., and Nicoud, F., 2015, "Uncertainty Quantification of Thermoacoustic Instabilities on a Swirled Stabilized Combustor," ASME Paper No. GT2015-44133.
[5] Tay-Wo-Chong, L., Bomberg, S., Ulhaq, A., Komarek, T., and Polifke, W., 2012, "Comparative Validation Study on Identification of Premixed Flame Transfer Function," ASME J. Eng. Gas Turbines Power, **134**(2), p. 021502.
[6] Bauerheim, M., Ndiaye, A., Constantine, P., Moreau, S., and Nicoud, F., 2016, "Symmetry Breaking of Azimuthal Thermoacoustic Modes: The UQ Perspective," J. Fluid Mech., **789**, pp. 534–566.
[7] Magri, L., Bauerheim, M., Nicoud, F., and Juniper, M. P., 2016, "Stability Analysis of Thermo-Acoustic Nonlinear Eigenproblems in Annular Combustors—Part II: Uncertainty Quantification," J. Comput. Phys., **325**, pp. 411–421.
[8] Silva, C., Magri, L., Runte, T., and Polifke, W., 2017, "Uncertainty Quantification of Growth Rates of Thermoacoustic Instability by an Adjoint Helmholtz Solver," ASME J. Eng. Gas Turbines Power, **139**(1), p. 011901.
[9] Blumenthal, R. S., Subramanian, P., Sujith, R., and Polifke, W., 2013, "Novel Perspectives on the Dynamics of Premixed Flames," Combust. Flame, **160**(7), pp. 1215–1224.
[10] Polifke, W., 2014, "Black-Box System Identification for Reduced Order Model Construction," Ann. Nucl. Energy, **67**, pp. 109–128.
[11] Sovardi, C., Jaensch, S., and Polifke, W., 2016, "Concurrent Identification of Aero-Acoustic Scattering and Noise Sources at a Flow Duct Singularity in Low Mach Number Flow," J. Sound Vib., **377**, pp. 90–105.
[12] Guo, S., Silva, C. F., Bauerheim, M., Ghani, A., and Polifke, W., 2018, "Evaluating the Impact of Uncertainty in Flame Impulse Response Model on Thermoacoustic Instability Prediction: A Dimensionality Reduction Approach," Proc. Combust. Inst. (in press).
[13] Constantine, P., Dow, E., and Wang, Q., 2014, "Active Subspace Methods in Theory and Practice: Applications to Kriging Surfaces," SIAM J. Sci. Comput., **36**(4), pp. A1500–A1524.
[14] Constantine, P. G., 2015, *Active Subspaces: Emerging Ideas in Dimension Reduction for Parameter Studies*, Vol. 2, SIAM, Philadelphia, PA.
[15] Lukaczyk, T. W., Constantine, P. G., Palacios, F., and Alonso, J. J., 2014, "Active Subspaces for Shape Optimization," AIAA Paper No. 2014-1171.
[16] Jefferson, J. L., Gilbert, J. M., Constantine, P. G., and Maxwell, R. M., 2015, "Active Subspaces for Sensitivity Analysis and Dimension Reduction of an Integrated Hydrologic Model," Comput. Geosci., **83**, pp. 127–138.
[17] Constantine, P. G., and Diaz, P., 2017, "Global Sensitivity Metrics From Active Subspaces," Reliab. Eng. Syst. Saf., **162**, pp. 1–13.
[18] Bodén, H., and Polifke, W., 2015, "Uncertainty Quantification Applied to Aeroacoustic Predictions," *Progress in Simulation, Control and Reduction of Ventilation Noise* (VKI Lecture Series 2015), C. Schram, ed., von Karman Institute for Fluid Dynamics, Sint-Genesius-Rode, Belgium.
[19] Keesman, K. J., 2011, "Time-Invariant System Identification," *System Identification* (Advanced Textbooks in Control and Signal Processing), Springer, London, pp. 59–167.
[20] Tay-Wo-Chong, L., Komarek, T., Kaess, R., Föller, S., and Polifke, W., 2010, "Identification of Flame Transfer Functions From LES of a Premixed Swirl Burner," ASME Paper No. GT2010-22769.
[21] Komarek, T., and Polifke, W., 2010, "Impact of Swirl Fluctuations on the Flame Response of a Perfectly Premixed Swirl Burner," ASME J. Eng. Gas Turbines Power, **132**(6), p. 061503.
[22] Emmert, T., Bomberg, S., Jaensch, S., and Polifke, W., 2017, "Acoustic and Intrinsic Thermoacoustic Modes of a Premixed Combustor," Proc. Combust. Inst., **36**(3), pp. 3835–3842.
[23] Cowan, G., 1998, *Statistical Data Analysis*, 1st ed., Clarendon Press, Gloucestershire, UK.
[24] Jaensch, S., Merk, M., Emmert, T., and Polifke, W., 2018, "Identification of Flame Transfer Functions in the Presence of Intrinsic Thermoacoustic Feedback and Noise," Combust. Theory Modell., **22**(3), pp. 613–634.
[25] Tangirala, A. K., 2014, *Principles of System Identification: Theory and Practice*, CRC Press, Boca Raton, FL.
[26] Avdonin, A., and Polifke, W., 2018, "Quantification of the Impact of Uncertainties in Operating Conditions on the Flame Transfer Function With Non-Intrusive Polynomial Chaos Expansion," ASME Paper No. GT2018-75476.